

Design and Analysis of a 2-DOF Compliant Mechanism for Nano Scale Positioning

Shyh-Chour Huang and Thanh-Phong Dao

Department of Mechanical Engineering, National Kaohsiung University of Applied Sciences, Kaohsiung, R.O.C, Taiwan

Copyright © 2015 ISSR Journals. This is an open access article distributed under the **Creative Commons Attribution License**, which permits unrestricted use, distribution, and reproduction in any medium, provided the original work is properly cited.

ABSTRACT: The paper investigates the design process and the analysis of a two degree of freedom compliant mechanism for nano scale positioning applications. In this research, the flexure based mechanism possesses a decoupled characteristic in x- and y motions and compact structure in size. Moreover, the mechanism's workspace will be amplified via using a lever amplification mechanism. In order to achieve an optimal size, a multiple objective optimization based on response surface method and kriging regression model are carried out. Besides, the effect of design variables on each of the output response of the proposed mechanism will analyzed as well. The proposed 2-DOF compliant mechanism size of $186\text{ mm} \times 186\text{ mm}$ possessed the workspace of $130\text{ }\mu\text{m} \times 130\text{ }\mu\text{m}$ in the x-and y axes. The confirmation experiment using a simulation in ANSYS revealed that the error between the predicted result and the actual value was about 1.6%. It means that there is a good agreement between two results. It is also clear that the proposed mechanism has much lower error than that of previous studies in the literature review. Ultimately, the proposed mechanism is expected to further applications in practice positioning and manipulator systems.

KEYWORDS: 2-DOF Compliant mechanism, Positioning, Manipulator, Multiple objective optimization.

1 BACKGROUND

Compliant mechanisms have been commonly used in high precision actuators, manipulators, robotics, and chemical environment to atomic microscopy, scanning devices, and turning and grinding machining. The reasons are that they possess monolithic topology, no friction, no lubricant, no need for maintenance, reduce assemble elements, and reduce time consuming for manufacturing. Hence, in the micro-and nano positioning technology, two axis monolithic mechanisms play an essential vital role.

2 INTRODUCTION

Nowadays, positioning systems and manipulators play more and more important roles in micro-and nano scale technology applications such as atomic microscopy, scanning device, bio-cell manipulator, turning machining, grinding, micro component assembly, optical fibers alignment, and medical device, etc. In order to fulfill such applications and desired requirements, the positioning stages and manipulators are preferred to be designed regarding to ultra high precision, resolution, high bandwidth.

Compliant mechanisms are the most potential candidate for designing such positioning stages due to monolithic structure, no need lubricant, no assembly, reduced time consuming. However, the design and analysis of a compliant mechanism have been challenging for engineers, scientists, researchers, and academic scholars. Howell [1] published a book to present some methods for design and analysis of compliant mechanisms. Huang et al. [2] designed and fabricated a microgripper with a topology optimal compliant mechanism. Recently, flexure based mechanisms were designed by Dao and Huang [3, 4].

In the past few decades, works related to single axis positioning and manipulator for scale nano technology was presented [5]. In addition, there have been a lot of great interests about two axis positioning systems [6-10]. Recently, a large

number of researchers have been paid their attention into design and analysis methodology of flexure based mechanisms such as flexibility matrix method [11], analysis approach [12, 13], and lumped model [14].

Previous studies focused on the establishment mathematic model of compliant mechanisms for positioning systems with good results. Even though the previous studies designed many suitable positioning stages; however, there has been large errors between models and simulation confirmation. In order to eliminate the error to adopted minum value, a computational analysis is developed in this study. Besides, a compact structure in size is a good prototype for nano scale positioning.

The current paper focuses on the design process and analysis a two degree of freedom (DOF) compliant mechanism for nano scale positioning. The proposed mechanism was developed including leaf springs and right circular hinges. Furthermore, the suggested mechanism can eliminate cross axis coupling between the x-and y axes. In this paper, the multiple objective optimization problem (MOO) was carried out to obtain an optimal size. Unlike previous studies, the MOO problem was based on the response surface approach and kiging regression. Finally, the effects of design variables on the output performances were also performed.

3 SIGNIFICANT AND CONTRIBUTION

The advantages of 2-DOF compliant mechanism for positioning systems and manipulators are ultra precision performance characteristics due to monolithic, high accurate, no joint, no friction, no clearance on backlash, no lubricant, and no maintenance. The proposed methodology is significant important to solve multiple objective optimization problem regarding to many input variables and output ones. It is expected to use in micro-and nano positioning technology and high precision manipulators.

4 MECHANICAL DESIGN

Aluminum 7075-T73 was chosen for the 2-DOF compliant mechanism due to their high yield strength-to-Young's modulus ratio. Young's modulus $E = 72$ GPa, yield strength $\sigma_y = 435$ MPa, Poisson rate $\nu = 0.33$, and density $\rho = 2810$ kg/m³. General, displacement-amplification mechanisms can be divided into two cases. One is a lever-type flexure hinge mechanism, as shown in Figs. 1a and 1b. In lever-type devices, the amplification ratio depends on the ratio o distances between pivots, and high transverse link stiffness is required. It needs relatively small number of flexure pivots, but the link size and high deformation are proportional to the amplification ratio, and hence high efficiency is hard to achieve.

The other is a bridge-type flexure hinge mechanism, as shown in Fig. 1c. The bridge-type flexure hinge mechanism needs high rigidity of link in longitudinal direction. It is relatively easy to design in compact and symmetric structure, but more flexure hinges are required than in lever-type mechanisms. Hence, this type was chosen for the mechanism.

In this study, a lever-type flexure hinge mechanism in Fig. 1a was preferred to be potential amplifier to enhance the workspace. Although the lever-type mechanism in Fig. 1b can obtain a larger workspace than that in Fig. 1a; however, the mechanism motion accuracy (resolution) of this type in Fig. 1b is lower than that in Fig. 1a.

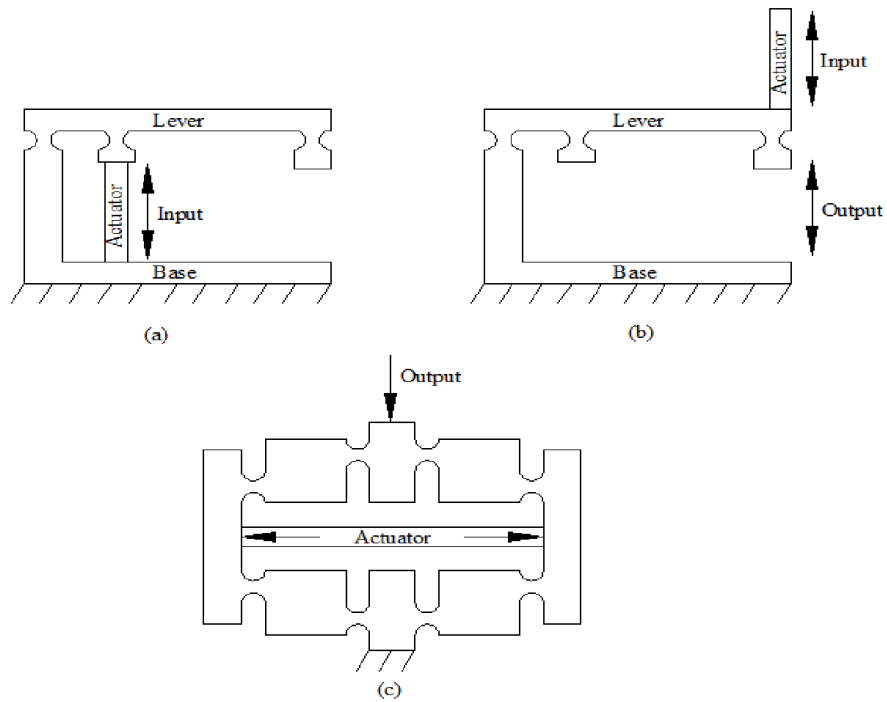


Fig. 1. Displacement-amplifier mechanisms: (a) and (b) lever type and (c) bridge type

The proposed x-and y axis compliant mechanism for positioning that can decouple two translational motions with a compact size was designed as in Fig. 2. The mechanism can amplify the displacement via using the aforementioned lever amplifier. In addition, the mechanism can eliminate the cross axis coupling between the x-and y axes.

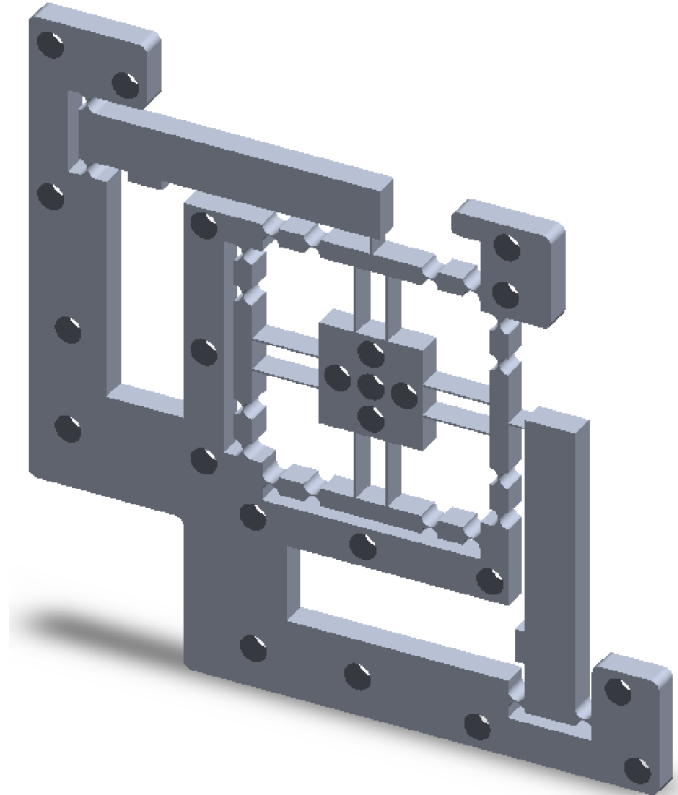


Fig. 2. 3-D Model of 2-DOF compliant mechanism for positioning in x-and y axes

5 METHODOLOGY

Prior to manufacture a prototype, multiple objective optimization (MOO) process should be performed by using various methods such as genetic algorithm, fuzzy logic reasoning, artificial neural networks, and hybrid procedures [15-17]. However, to speed a fast manufacturing process as well as reduce time consuming, in this research the response surface method and kiging regression model were used in ANSYS software. This is a symmetric compliant mechanism, hence during the analysis process, the research concentrated on an exerting force F in the y-axis.

According to the amount of design variables, the number of experiments is identified by utilizing the central composite design (CCD) method. Subsequently, computational analyses are performed to obtain the characteristics of the above design points, such as the workspace. As these characteristics are dependent on the design variables, they are named as the output parameters. A response surface is a statistical regression model characterizing the relationships between the output parameter and the design variables. Based on the computational results, a response surface can be created for each output parameter. A 2-D dimension diagram for the positioning mechanism is shown in Fig. 3.

In this paper, in the design of experiments, seven-factor five-level CCD with rotatable design was used. The number of experiments required by the CCD is described by the following equation:

$$N = 2^{(k-f)} + 2k + n_c \quad (1)$$

where N is the total number of experiments, k is the number of design variables, f is the factorial number, and n_c is the number of replicates at the center point of the design space.

In this paper, $k = 4$ and in this case, the factorial number is $f = 1$. For the computational analysis, only one replicate is required at the center point, i.e., $n_c = 1$.

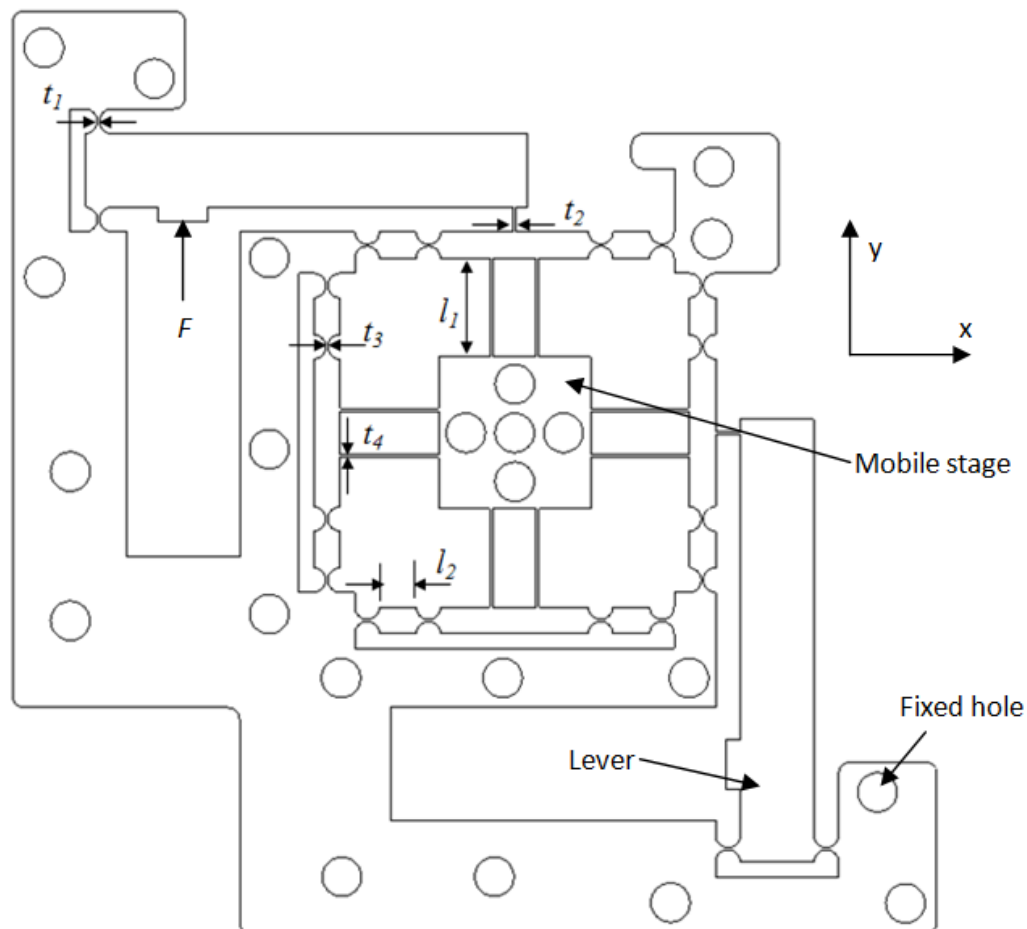


Fig. 3. 2-D dimension view of the 2-DOF compliant mechanism for positioning (unit:mm)

In this section, the goal driven optimization toolbox in ANSYS is performed to optimize and control design parameters. Multiple objective optimizations briefly describes as follows:

- Maximize displacement of the platform up to more than 100µm
- Maximize first natural frequency up to more than 590 HZ
- Minimize equivalent stress
- Safety factor is constrained to be more than 1.8

Subject to constrains as follows:

- Thickness of circular hinge $0.3mm \leq t_1 \leq 0.8mm$
- Thickness of leaf spring $0.3mm \leq t_2 \leq 0.8mm$
- Thickness of circular hinge $0.3mm \leq t_3 \leq 0.8mm$
- Thickness of leaf spring $0.3mm \leq t_4 \leq 0.8mm$
- Radius of circular hinge $2.5mm$
- Width of decoupled element $7.44mm$
- Width of kinematic chain $20mm$
- Thickness of lever $15mm$
- Effective stress $\sigma \leq \sigma_y / \eta$

where σ_y denotes the yield strength of the adopted material, and $\eta \in (1, \infty)$ is specified safety factor. In this paper, η is selected as 1.8.

The coded levels for the design variables are given in Table 1. The 25 design points were computed via using Eq. (1) for the design of experiments, as listed in Table 2.

Table 1. Coded levels of the design variables

Design variable	Symbol	Coded levels				
		-c	-b	a	b	c
t₁ (mm)	x ₁	0.3	0.4	0.5	0.6	0.7
t₂ (mm)	x ₂	0.3	0.4	0.5	0.6	0.7
t₃ (mm)	x ₃	0.3	0.4	0.5	0.6	0.7
t₄ (mm)	x ₄	0.3	0.4	0.5	0.6	0.7

Table 2. Design of experiments

No.	x_1	x_2	x_3	x_4
1	0.5	0.5	0.5	0.5
2	0.5	0.5	0.5	0.3
3	0.5	0.5	0.5	0.7
4	0.3	0.5	0.5	0.5
5	0.7	0.5	0.5	0.5
6	0.5	0.3	0.5	0.5
7	0.5	0.7	0.5	0.5
8	0.5	0.5	0.3	0.5
9	0.5	0.5	0.7	0.5
10	0.4	0.4	0.4	0.4
11	0.4	0.4	0.4	0.6
12	0.6	0.4	0.4	0.4
13	0.6	0.4	0.4	0.6
14	0.4	0.6	0.4	0.4
15	0.4	0.6	0.4	0.6
16	0.6	0.6	0.4	0.4
17	0.6	0.6	0.4	0.6
18	0.4	0.4	0.6	0.4
19	0.4	0.4	0.6	0.6
20	0.6	0.4	0.6	0.4
21	0.6	0.4	0.6	0.6
22	0.4	0.6	0.6	0.4
23	0.4	0.6	0.6	0.6
24	0.6	0.6	0.6	0.4
25	0.6	0.6	0.6	0.6

6 RESULTS AND DISCUSSION

Based on the computational results in Table 3, a response surface was created for each output response. Table 4 shows the goodness of fit of the response surfaces. Fig. 4 indicates the comparison between the output parameters predicted from the response surfaces and those observed at the design points. Excellent agreements demonstrate the effectiveness of the response surfaces. Figs. 5 and 6 provide the effect plots, showing the influence of the design variables on the output parameters at the center point of the design space. Referring Fig. 5a, the maximum displacement is very sensitive to t_3 , while the influence of t_4 is two much low, and the other design variables is moderate. In Fig. 5b, it is seen that the maximum equivalent stress is t_1 and t_3 , while the influence of t_4 is two much low, and the other design variable is moderate. With regard to Fig. 6a, it is clear that the safety factor is very sensitive to t_1 and t_3 , while the influence of t_4 is two much low, and the other design variable is moderate. Regarding to Fig. 6b, it indicates that the first natural frequency is very sensitive to t_1 and t_3 , while the influence of t_4 is two much low, and the other design variable is moderate.

Table 3. Design layout plan and computational results

No.	(x ₁ , x ₂ , x ₃ , x ₄)	y ₁ (μm)	y ₂ (MPa)	y ₃ (η)	y ₄ (Hz)
1	(a, a, a, a)	172.73	229.44	1.90	596.44
2	(a, a, a, -c)	175.45	231.79	1.88	592.42
3	(a, a, a, c)	167.66	226.35	1.92	604.12
4	(-c, a, a, a)	119.12	244.89	1.78	730.53
5	(c, a, a, a)	95.68	149.41	2.91	707.41
6	(a, -c, a, a)	174.98	230.17	1.89	596.24
7	(a, c, a, a)	169.98	228.67	1.90	596.24
8	(a, a, -c, a)	223.40	266.14	1.63	527.78
9	(a, a, c, a)	77.31	126.73	3.43	763.49
10	(-b, -b, -b, -b)	107.67	151.60	2.87	739.69
11	(-b, -b, -b, b)	120.69	151.48	2.87	715.92
12	(b, -b, -b, -b)	97.94	128.90	3.37	755.23
13	(b, -b, -b, b)	121.32	154.36	2.82	709.07
14	(-b, b, -b, -b)	121.17	160.88	2.70	702.01
15	(-b, b, -b, b)	108.42	148.60	2.93	733.25
16	(b, b, -b, -b)	103.17	151.62	2.87	714.80
17	(b, b, -b, b)	112.06	146.37	2.97	740.26
18	(-b, -b, b, -b)	168.09	228.06	1.91	555.33
19	(-b, -b, b, b)	164.60	221.02	1.97	560.86
20	(b, -b, b, -b)	147.74	208.28	2.09	555.24
21	(b, -b, b, b)	144.72	201.54	2.16	560.89
22	(-b, b, b, -b)	165.54	221.96	1.96	554.77
23	(-b, b, b, b)	162.21	215.59	2.02	560.34
24	(b, b, b, -b)	87.54	134.21	3.24	736.28
25	(b, b, b, b)	149.41	201.59	2.16	556.65

When the response surfaces have been built, the lower and upper bounds of the response surfaces are listed in Table 5. It was observed that in the current design space, all the design objectives as above section are achievable. Consequently, the computational optimization would be performed based on established response surfaces.

Table 4. The goodness of fit of the response surfaces

	Workspace	Equivalent Stress	Safety factor	First natural frequency
Coefficient of Determination (Best Value = 1)	1	1	1	1
Maximum Relative Residual (Best Value = 0%)	0	0	0	0
Root Mean Square Error (Best Value = 0)	4*10 ⁻⁹	5*10 ⁻⁶	3*10 ⁻⁸	7*10 ⁻⁶
Relative Root Mean Square Error (Best Value = 0%)	0	0	0	0
Relative Maximum Absolute Error (Best Value = 0%)	0	0	0	0
Relative Average Absolute Error (Best Value = 0%)	0	0	0	0

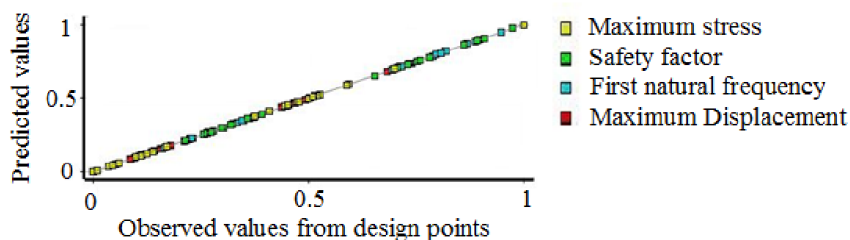


Fig. 4. Goodness of fit of the response surfaces and the design points

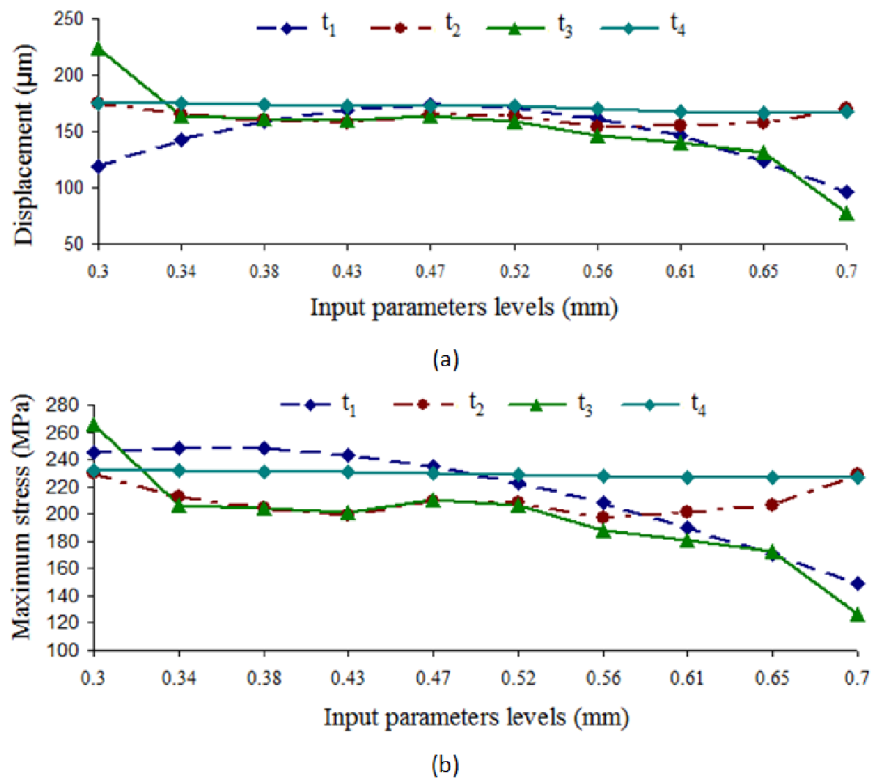
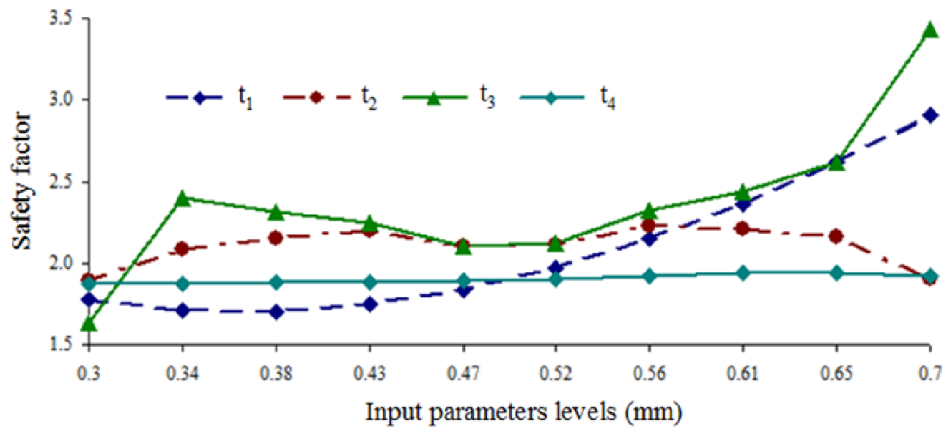
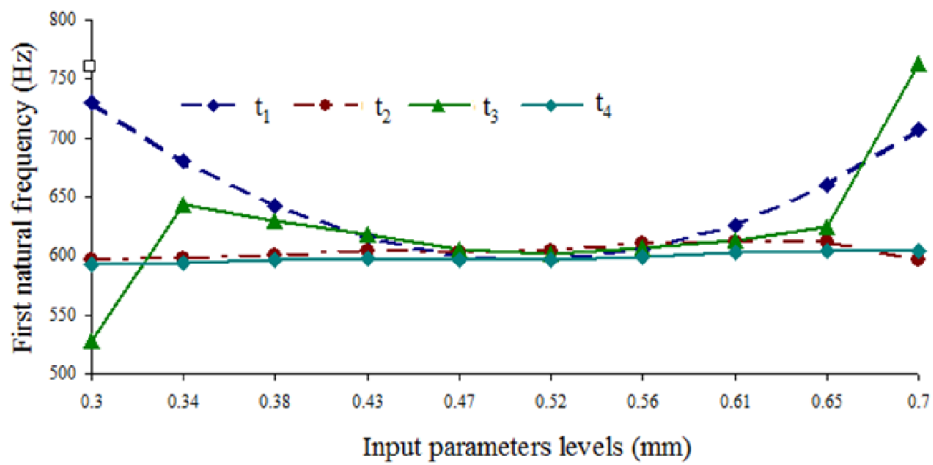


Fig. 5. Effect diagram: (a) maximum displacement, (b) maximum equivalent stress



(a)



(b)

Fig. 6. Effect plot of: (a) safety factor, (b) first natural frequency

Table 5. Bounds of the response surfaces

Characteristics	Minimum	Maximum	Unit
Maximum displacement	44.91	192.67	μm
Maximum stress	17.657	269.78	MPa
First natural frequency	528.75	1029.20	Hz
Safety factor	1.43	5.01	

However, this workspace is not pursued in this study, the monolithic stage is expected to provide a workspace range in excess of $100\mu\text{m} \times 100\mu\text{m}$. Based on Table 5, the design objectives can be refined to be:

- (1) The maximum displacement should be around $130\mu\text{m}$
- (2) The maximum equivalent stress should be around 230MPa
- (3) The first natural frequency should be around 650Hz
- (4) The safety factor should be around 1.8.

Referring to subsequent iterations, it is noted that even though the change the weight and priority of various objectives, the results are not changed. On the other word, whole the further results are similar the ones of the first three iterations. Hence, this work only carries on the first three iterations. Three best candidates are recorded in Table 6. Ultimately, the candidate 2 is selected as the optimal design because it completely satisfies the four design objectives. Another reason is that

the higher first natural frequency can increase the speed of the 2-DOF compliant mechanism, as seen in the candidate 2 (663.26 Hz).

Table 6. Comparisons among candidates

Coded levels	Candidate 1	Candidate 2	Candidate 3
x_1 (mm)	0.30	0.32	0.30
x_2 (mm)	0.53	0.62	0.60
x_3 (mm)	0.42	0.38	0.54
x_4 (mm)	0.31	0.37	0.35
y_1 (μm)	139.63	131.60	131.67
y_2 (MPa)	227.69	227.34	223.18
y_3 (Hz)	656.02	663.26	659.18
y_4	1.81	1.95	1.89

7 CONFIRMATION EXPERIMENT

A confirmation simulation in ANSYS software can replace a real experiment that was conducted in order to evaluate the predicted travel range in the y-axis. As shown in Fig. 7, the travel of the 2-DOF compliant mechanism was $133.82 \mu\text{m}$ while the predicted travel of the candidate 2 in Table 6 was $131.60 \mu\text{m}$. The deviation error between the predicted value and actual value is 1.6%.

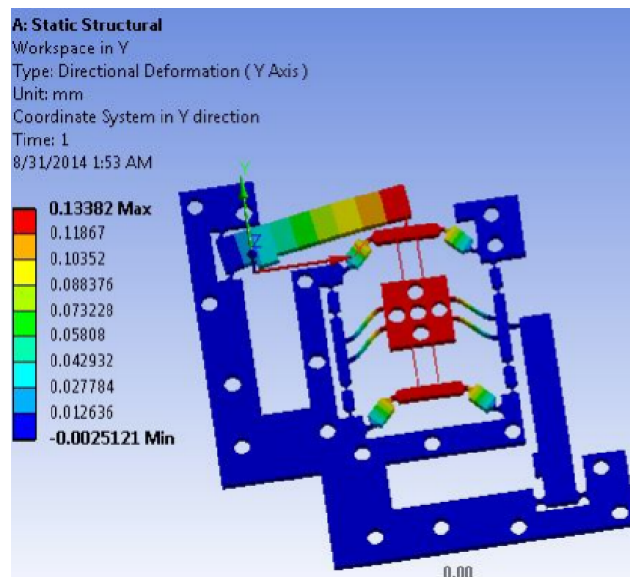


Fig. 7. The travel of the 2-DOF compliant mechanism in the y-axis

8 CONCLUSION

This research presented the design and analysis of two axis translational compliant mechanism for nano scale positioning. In this paper, the proposed mechanism was designed via the use of the concept of compliant mechanism. And then multiple objective optimization problem of the mechanism was performed by using the response surface method and kriging regression model in ANSYS software. A finite element analysis was conducted to explore the effects of process parameters on the displacement, stress, first natural frequency, and safety factor. The results showed that the mechanism can amplify the workspace by its self. The proposed 2-DOF compliant mechanism size of $186 \text{ mm} \times 186 \text{ mm}$ possessed the workspace of $130 \mu\text{m} \times 130 \mu\text{m}$ in the x-and y axes. The confirmation experiment using simulation in ANSYS revealed that the error between the predicted result and actual value was 1.6%. It means that there is a good agreement between two results. It is also clear that the proposed mechanism has much lower error than that of previous studies in the literature review.

Future work will conclude investigation into the suitable controller design to control nonlinear characteristics. A prototype will be manufactured and evaluated by experimental tests. The proposed mechanism is expected to be good potential candidate for atomic microscopy and micro-and nano scale technologies.

REFERENCES

- [1] L.L. Howell, *Compliant mechanisms*, New York, Wiley, 2001.
- [2] S.C. Huang, C.C. Chiu, and W.L. Chen, "Design and fabrication of a microgripper with a topology optimal compliant mechanism," *Int. J. Computational Materials Science and Surface Engineering*, vol. 2, No. ¾, pp. 282–301, 2009.
- [3] T.P. Dao and S.C. Huang, "Development and Optimization of a Compliant Clamp for Grasping Robotics," *International Journal of Innovation and Applied Studies*, vol. 7, No. 1, pp. 231–238, 2014.
- [4] T.P. Dao and S.C. Huang, "Design and Dynamic Analysis of a Parallel Compliant Vibration Mechanism for High Precision Production Line," *International Journal of Innovation and Scientific Research*, vol. 8, No. 2, pp. 118–123, 2014.
- [5] S.-C. Chen and M. L. Culpepper, "Design of a six-axis micro-scale nanopositioner—µhexflex," *Precis. Eng.*, vol. 30, pp. 314–324, 2006.
- [6] Y.M. Li and Q.S Xu, "Design and Analysis of a Totally Decoupled Flexure-Based XY Parallel Micromanipulator," *IEEE TRANSACTIONS ON ROBOTICS*, vol. 25, No. 3, pp. 645–657, 2009.
- [7] Y.M. Li and Q.S Xu, "A Novel Piezoactuated XY Stage With Parallel, Decoupled, and Stacked Flexure Structure for Micro-/Nanopositioning," *IEEE TRANSACTIONS ON INDUSTRIAL ELECTRONICS*, vol. 58, No. 8, 3601–3615, 2011.
- [8] Y.M. Li, J.M Huang, and H. Tang, "A Compliant Parallel XY Micromotion Stage With Complete Kinematic Decoupling," *IEEE TRANSACTIONS ON AUTOMATION SCIENCE AND ENGINEERING*, Vol. 9, No. 3, pp. 538–553, 2012.
- [9] Y.M. Li and Q.S Xu, "A Novel Design and Analysis of a 2-DOF Compliant Parallel Micromanipulator for Nanomanipulation," *IEEE TRANSACTIONS ON AUTOMATION SCIENCE AND ENGINEERING*, Vol. 3, No. 3, pp. 247–254, 2006.
- [10] Q.S. Xu, "Design and Development of a Compact Flexure-Based XY Precision Positioning System with Centimeter Range," *IEEE TRANSACTIONS ON INDUSTRIAL ELECTRONICS*, Vol. 61, No. 2, 2014.
- [11] Y.M. Li, S.L. Xiao, L.Q. Xi, and Z.G. Wu, "Design, Modeling, Control and Experiment for a 2-DOF Compliant Micro-Motion Stage," *International Journal of Precision Engineering and Manufacturing*, vol. 15, No. 4, pp. 735-744.
- [12] S. Polit and J. Dong, "Development of a High-Bandwidth XY, Nanopositioning Stage for High-Rate, Micro-/Nanomanufacturing," *IEEE/ASME TRANSACTIONS ON MECHATRONICS*," Vol. 16, No. 4, pp. 724–733, 2011.
- [13] H. Tang and Y.M. Li, "Optimal Design, Modeling and Analysis of a 2-DOF Nanopositioning Stage with Dual-Mode: Towards High-Rate AFM Scanning," in *Proceedings of IEEE/RSJ International Conference on Intelligent Robots and Systems Vilamoura, Algarve, Portugal*, pp. 658–663, October 7-12, 2012.
- [14] Y.M. Li and Q.S Xu, "Optimum Design and Development of an XY Flexure Micromanipulator for Micro Scale Positioning," *2008 IEEE International Conference on Robotics and Automation Pasadena, CA, USA*, pp. 3112–3117, May 19-23, 2008.
- [15] T.P. Dao and S.C. Huang, "Design and Analysis of a Clothes Holding Flexible Mechanism" *Journal of Engineering Technology and Education*, vol. 11, No. 1, pp. 70–78, 2014.
- [16] T.P. Dao and S.C. Huang, "An Optimal Study of a Gripper Compliant Mechanism Based on Fuzzy-Taguchi Method," *Applied Mechanics and Materials*, vol. 418, pp 141–144, 2013.
- [17] T.P. Dao and S.C. Huang, "Study on Optimization for Four Bar-Partially Compliant Mechanism," *Journal of Engineering Technology and Education*, vol. 10, No. 4, pp. 433–449.